

Two Motors Drive System Topologies with Five-Leg Inverter

E. C. dos Santos Jr.¹, C. B. Jacobina¹, O. I. da Silva ² and A. M. N. Lima¹

¹Departamento de Engenharia Elétrica
Universidade Federal de Campina Grande
Campina Grande - PB - Brazil
²IFET Recife - PE - Brazil

Abstract- This paper presents three motor drive system topologies using five-leg converters. The proposed configurations present lower dc-link voltage than their counterparts found in the literature. All the topologies use ten power switches and does not have any connection to the mid-point of the capacitor bank. Model, pulse-width modulation techniques and control strategies are investigated. The main characteristics of the drive systems are also presented. Experimental and simulated results demonstrate the feasibility of the systems.

I. INTRODUCTION

To feed and control independently multiple ac motors in industrial applications usually require to use multiple variable frequency drive systems. An alternative to reduce the installation cost is to use converter topologies that allow to reduce the number of power switching devices [1–8].

The five-leg converter topology for supplying two ac motors independently has been used as a solution for driving a three-phase induction motor for traction and a two-phase induction motor for compression in automotive applications [9], [10]. This solution has allowed to reduce the cost of drive system for the compressor motor [9], [10]. The use of the five five-leg inverter topology for supplying two motors has also been investigated in [11], [12], for three-phase motors and two-phase motors connected in parallel and series arrangements, respectively. Figs. 1(a) and 1(b) shows the configurations of the two systems studied in [11] and [12] with three-phase motors.

This paper presents three configurations of motor drive systems based on the five-leg inverter topology. In this paper only three-phase motors were considered, each one connected in a wye or delta arrangement, as it can be observed in Fig. 2. Fig. 2(a) shows the Configuration YD-P, which means wye (Y) and delta (D) arrangement of the three-phase motors being connected in a parallel (P). Figs. 2(b) and 2(c) show the Configurations DD-P and YD-S, respectively.

All the proposed configurations are composed of switches $q_1, \bar{q}_1, q_2, \bar{q}_2, q_3, \bar{q}_3, q_4, \bar{q}_4, q_5$ and \bar{q}_5 . The switch-pairs $q_1 - \bar{q}_1, q_2 - \bar{q}_2, q_3 - \bar{q}_3, q_4 - \bar{q}_4$ and $q_5 - \bar{q}_5$ are complementary. The conduction state of all switches can be represented by

binary variable q_1, q_2, q_3, q_4 and q_5 , where $q = 1$ indicates a closed switch while $q = 0$ indicates an open one.

II. THREE-PHASE MOTOR MODEL

A typical three-phase motor has been used in this work. Selecting a fixed coordinate reference frame, the mathematical model that describes the dynamic behavior of the three-phase induction motor is given by

$$\mathbf{v}_{sdq} = r_s \mathbf{i}_{sdq} + \frac{d}{dt} \boldsymbol{\lambda}_{sdq} \quad (1)$$

$$\mathbf{v}_{rdq} = r_r \mathbf{i}_{rdq} + \frac{d}{dt} \boldsymbol{\lambda}_{rdq} - j\omega_r \boldsymbol{\lambda}_{rdq} \quad (2)$$

$$\boldsymbol{\lambda}_{sdq} = l_s \mathbf{i}_{sdq} + l_{sr} \mathbf{i}_{rdq} \quad (3)$$

$$\boldsymbol{\lambda}_{rdq} = l_{sr} \mathbf{i}_{sdq} + l_r \mathbf{i}_{rdq} \quad (4)$$

$$v_{so} = r_s i_{so} + l_{ls} \frac{d}{dt} i_{so} \quad (5)$$

$$v_{ro} = r_r i_{ro} + l_{lr} \frac{d}{dt} i_{ro} \quad (6)$$

$$T_e = Pl_{sr}(i_{sq}i_{rd} - i_{sd}i_{rq}). \quad (7)$$

where $\mathbf{v}_{sdq} = v_{sd} + jv_{sq}$, $\mathbf{i}_{sdq} = i_{sd} + ji_{sq}$, and $\boldsymbol{\lambda}_{sdq} = \lambda_{sd} + j\lambda_{sq}$ are the voltage, current and flux dq vectors of the stator, respectively; v_{so} and i_{so} are the homopolar voltage and current of the stator, respectively (the equivalent rotor variables are obtained by replacing the subscript s by r); T_e is the electromagnetic torque; ω_r is the angular frequency of the rotor; r_s and r_r are the stator and rotor resistances; l_s, l_{ls}, l_r and l_{lr} are the self and leakage inductance of the stator and rotor, respectively; l_{sr} is the mutual inductance and P is the number of pair of poles of the machine.

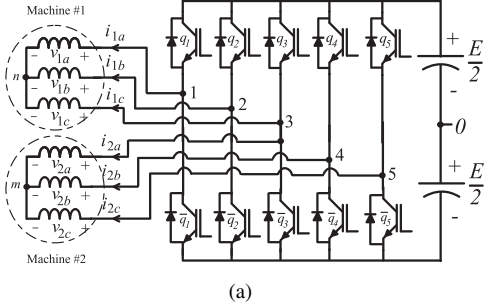
The dqo stator variables of the previous model can be determined from the abc variables by using the transformation given by

$$\mathbf{w}_{sabc} = \mathbf{A}_s \mathbf{w}_{sdqo} \quad (8)$$

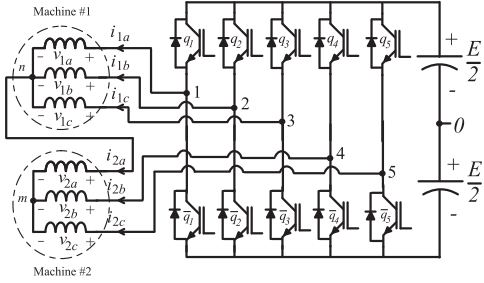
with $\mathbf{w}_{sabc} = [w_{sa} \ w_{sb} \ w_{sc}]^T$, $\mathbf{w}_{sdqo} = [w_{sd} \ w_{sq} \ w_{so}]^T$ and

$$\mathbf{A}_s = \sqrt{\frac{2}{3}} \begin{bmatrix} 1 & 0 & \frac{\sqrt{2}}{2} \\ -\frac{1}{2} & \frac{\sqrt{3}}{2} & \frac{\sqrt{2}}{2} \\ -\frac{1}{2} & -\frac{\sqrt{3}}{2} & \frac{\sqrt{2}}{2} \end{bmatrix}$$

Vectors \mathbf{w}_{sabc} and \mathbf{w}_{sdqo} can be voltage or current or flux vectors and $\mathbf{A}_s^{-1} = \mathbf{A}_s^T$.



(a)



(b)

Fig. 1. Five leg converter configurations studied in [11] and [12]: (a) Configuration YY-P and (b) Configuration YY-S.

III. CONFIGURATION YD-P

A. Model

The Configuration YD-P is composed of two three-phase motors arranged in a wye and delta connection and sharing the leg 3 ($q_3-\bar{q}_3$) [see Fig. 2(a)]. The motors voltages are given by

$$v_{1a} = v_{10} - v_{n0} \quad (9)$$

$$v_{1b} = v_{20} - v_{n0} \quad (10)$$

$$v_{1c} = v_{30} - v_{n0} \quad (11)$$

$$v_{2a} = v_{40} - v_{30} \quad (12)$$

$$v_{2b} = v_{50} - v_{40} \quad (13)$$

$$v_{2c} = v_{30} - v_{50}. \quad (14)$$

Applying the transformation given in (8), the dq voltages associated with the machine 1 (wye connected) are given by:

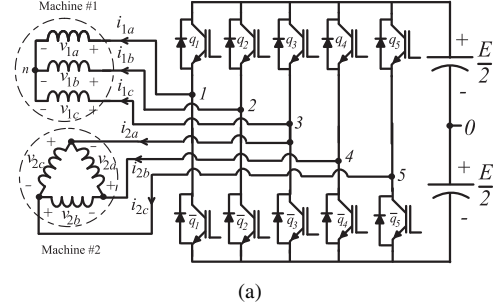
$$v_{1d} = \sqrt{\frac{2}{3}} \left(v_{10} - \frac{1}{2}v_{20} - \frac{1}{2}v_{30} \right) \quad (15)$$

$$v_{1q} = \frac{1}{\sqrt{2}} (v_{20} - v_{30}) \quad (16)$$

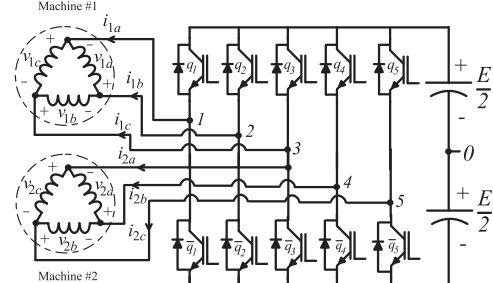
while, the dq voltages associated with the machine 2 (Δ connected) are given by:

$$v_{2d} = \sqrt{\frac{3}{2}} (v_{40} - v_{30}) \quad (17)$$

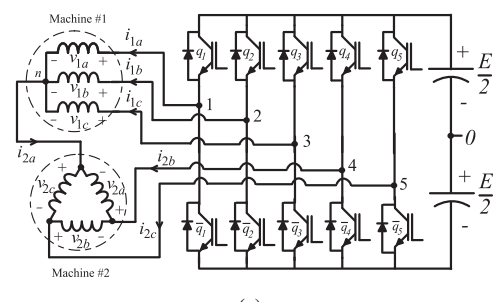
$$v_{2q} = \frac{1}{\sqrt{2}} (2v_{50} - v_{40} - v_{30}). \quad (18)$$



(a)



(b)



(c)

Fig. 2. Proposed five leg converter configurations: (a) Configuration YD-P, (b) Configuration DD-P, (c) Configuration YD-S.

B. PWM Strategy

From (9)-(14), it can be written for the reference voltages

$$v_{1a}^* = v_{10}^* - v_{n0}^* \quad (19)$$

$$v_{1b}^* = v_{20}^* - v_{n0}^* \quad (20)$$

$$v_{1c}^* = v_{30}^* - v_{n0}^* \quad (21)$$

$$v_{2a}^* + v_{1c}^* = v_{40}^* - v_{n0}^* \quad (22)$$

$$v_{1c}^* - v_{2c}^* = v_{50}^* - v_{n0}^*. \quad (23)$$

In this equations the reference voltages (v_{1a}^* , v_{1b}^* , v_{1c}^* , v_{2a}^* , and v_{2c}^*) are expressed in terms of dq reference voltages (v_{1d}^* , v_{1q}^* ,

v_{2d}^* , and v_{2q}^*) defined by the controllers, as follows

$$v_{1a}^* = \sqrt{\frac{2}{3}} v_{1d}^* \quad (24)$$

$$v_{1b}^* = -\sqrt{\frac{1}{6}} v_{1d}^* + \sqrt{\frac{1}{2}} v_{1q}^* \quad (25)$$

$$v_{1c}^* = -\sqrt{\frac{1}{6}} v_{1d}^* - \sqrt{\frac{1}{2}} v_{1q}^* \quad (26)$$

$$v_{2a}^* = \sqrt{\frac{2}{3}} v_{2d}^* \quad (27)$$

$$v_{2c}^* = -\sqrt{\frac{1}{6}} v_{2d}^* - \sqrt{\frac{1}{2}} v_{2q}^*. \quad (28)$$

The reference pole voltages can be obtained directly from (19)-(23), that is,

$$v_{10}^* = v_{1a}^* + v_{n0}^* \quad (29)$$

$$v_{20}^* = v_{1b}^* + v_{n0}^* \quad (30)$$

$$v_{30}^* = v_{1c}^* + v_{n0}^* \quad (31)$$

$$v_{40}^* = v_{2a}^* + v_{1c}^* + v_{n0}^* \quad (32)$$

$$v_{50}^* = v_{1c}^* - v_{2c}^* + v_{n0}^*. \quad (33)$$

Notice (29)-(33) cannot be solved unless v_{n0}^* is specified.

The voltage v_{n0}^* can be calculated taking into account the general apportioning factor μ that is

$$v_{n0}^* = E(\mu - \frac{1}{2}) - \mu v_{\max}^* + (\mu - 1)v_{\min}^*. \quad (34)$$

where $v_{\max}^* = \max V$ and $v_{\min}^* = \min V$, where $V = \{v_{1a}^*, v_{1b}^*, v_{1c}^*, v_{2a}^* + v_{1c}^*, v_{1c}^* - v_{2c}^*\}$.

Expression (34) was derived by using the same approach employed to derive the equivalent one for the three-phase PWM modulator [13], [14].

Given the pole voltage determined in the previous equations, it is possible to calculate the pulse-widths τ_1 to τ_5 by using

$$\tau_l = \frac{T}{2} + \frac{T}{E} v_{n0}^* \text{ for } l = 1 \text{ to } 5$$

and then program the timers accordingly.

Alternatively, the gating signals can be obtained by comparison of the pole voltages with a high frequency triangular carrier signal.

IV. CONFIGURATION DD-P

A. Model

The Configuration DD-P is composed of two three-phase motors arranged in a delta connection and sharing the leg 3 ($q_3-\bar{q}_3$) [see Fig. 2(b)]. The motors voltages are given by

$$v_{1a} = v_{20} - v_{10} \quad (35)$$

$$v_{1b} = v_{30} - v_{20} \quad (36)$$

$$v_{1c} = v_{10} - v_{30} \quad (37)$$

$$v_{2a} = v_{40} - v_{30} \quad (38)$$

$$v_{2b} = v_{50} - v_{40} \quad (39)$$

$$v_{2c} = v_{30} - v_{50}. \quad (40)$$

Applying the transformation matrix given in (8), the dq voltages associated with the machine 1 are given by:

$$v_{1d} = \sqrt{\frac{3}{2}} (-v_{10} + v_{20}) \quad (41)$$

$$v_{1q} = \frac{1}{\sqrt{2}} (2v_{30} - v_{20} - v_{10}) \quad (42)$$

while, the dq voltages associated with the machine 2 are given by:

$$v_{2d} = \sqrt{\frac{3}{2}} (-v_{30} + v_{40}) \quad (43)$$

$$v_{2q} = \frac{1}{\sqrt{2}} (2v_{50} - v_{40} - v_{30}). \quad (44)$$

B. PWM Strategy

From (35)-(40) it can be written for the reference voltages

$$v_{1a}^* = v_{20}^* - v_{10}^* \quad (45)$$

$$-v_{1c}^* = v_{30}^* - v_{10}^* \quad (46)$$

$$v_{2a}^* - v_{1c}^* = v_{40}^* - v_{10}^* \quad (47)$$

$$-v_{2c}^* - v_{1c}^* = v_{50}^* - v_{10}^*. \quad (48)$$

Introducing an auxiliary variable v_n^* , the reference pole voltages can be obtained directly from (45)-(48), that is,

$$v_{10}^* = v_n^* \quad (49)$$

$$v_{20}^* = v_{1a}^* + v_n^* \quad (50)$$

$$v_{30}^* = -v_{1c}^* + v_n^* \quad (51)$$

$$v_{40}^* = v_{2a}^* - v_{1c}^* + v_n^* \quad (52)$$

$$v_{50}^* = -v_{2c}^* - v_{1c}^* + v_n^*. \quad (53)$$

The voltage v_n^* is obtained using the same approach employed for Configuration YD-P for v_{n0}^* . The expression (34) is still valid with $V = \{0, v_{1a}^*, -v_{1c}^*, v_{2a}^* - v_{1c}^*, -v_{2c}^* - v_{1c}^*\}$.

V. CONFIGURATION YD-S

A. Model

The Configuration YD-S is composed of two three-phase motors arranged in a series connection, without sharing any leg [see Fig. 2(c)]. The motors voltages are given by

$$v_{1a} = v_{10} - v_{n0} \quad (54)$$

$$v_{1b} = v_{20} - v_{n0} \quad (55)$$

$$v_{1c} = v_{30} - v_{n0} \quad (56)$$

$$v_{2a} = v_{40} - v_{n0} \quad (57)$$

$$v_{2b} = v_{50} - v_{40} \quad (58)$$

$$v_{2c} = v_{n0} - v_{50}. \quad (59)$$

Applying the transformation matrix given in (8), the odq voltages associated with the machine 1 are given by:

$$v_{1d} = \sqrt{\frac{2}{3}} \left(v_{10} - \frac{1}{2} v_{20} - \frac{1}{2} v_{30} \right) \quad (60)$$

$$v_{1q} = \frac{1}{\sqrt{2}} (v_{20} - v_{30}) \quad (61)$$

$$v_{1o} = \frac{1}{\sqrt{3}} [(v_{10} + v_{20} + v_{30}) - 3v_{n0}] \quad (62)$$

The voltage v_{n0} can be written as follows:

$$v_{n0} = \frac{1}{3} (v_{10} + v_{20} + v_{30}) - \frac{\sqrt{3}}{3} v_{1o} \quad (63)$$

From the homopolar model and considering the homopolar current of machine 1 equal to $i_{2a}/\sqrt{3}$ it follow that

$$v_{1o} = r_s \frac{i_{2a}}{\sqrt{3}} + l_{ls} \frac{d}{dt} \frac{i_{2a}}{\sqrt{3}} \quad (64)$$

The dq voltages associated with the machine 2 are given by

$$v_{2d} = \left(\frac{2}{\sqrt{3}} + \frac{1}{\sqrt{6}} \right) (v_{40} - v_{n0}) \quad (65)$$

$$v_{2q} = \frac{1}{\sqrt{2}} (2v_{50} - v_{40} - v_{n0}) \quad (66)$$

B. PWM Strategy

From (54)-(59) it can be written for the reference pole voltages

$$\begin{aligned} v_{10}^* &= v_{1a}'^* + v_{n0}^* \\ v_{20}^* &= v_{1b}'^* + v_{n0}^* \\ v_{30}^* &= v_{1c}'^* + v_{n0}^* \\ v_{40}^* &= v_{2a}'^* + v_{n0}^* \\ v_{50}^* &= -v_{2c}'^* + v_{n0}^* \end{aligned}$$

where $v_{1a}'^* = v_{1a}^* + \frac{1}{\sqrt{3}} v_{1o}^*$, $v_{1b}'^* = v_{1b}^* + \frac{1}{\sqrt{3}} v_{1o}^*$, $v_{1c}'^* = v_{1c}^* + \frac{1}{\sqrt{3}} v_{1o}^*$; with v_{1o}^* obtained from the homopolar model [see (64)].

The voltage v_{n0}^* is obtained using the same approach employed for Configuration YD-P. The expression (34) is still valid with $V = \{v_{1a}'^*, v_{1b}'^*, v_{1c}'^*, v_{2a}'^*, -v_{2c}'^*\}$.

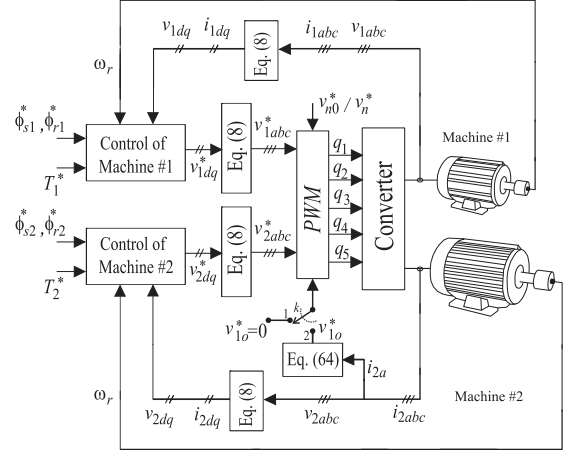
VI. CONTROL STRATEGY

The control block diagram of the Configurations YD-P and DD-P are shown in Fig. 3(a) with the switch k connected to point 1 ($k \rightarrow 1$). The control block diagram of the Configuration YD-S is shown in Fig. 3(a) with the switch k connected to point 2 ($k \rightarrow 2$). The Control of Machine blocks shown Fig. 3(a) can be implemented by controlling the dq currents (as in field-oriented strategy), the dq magnetic flux (as in direct torque strategy) or the dq voltages (as in the volts-per-hertz strategy). The dc-link voltage is obtained from a utility grid through a rectifier circuit. In application where the utility grid is not available, as in automotive and ships applications, the dc-link voltage can be imposed by a dc-dc converter connected to a battery.

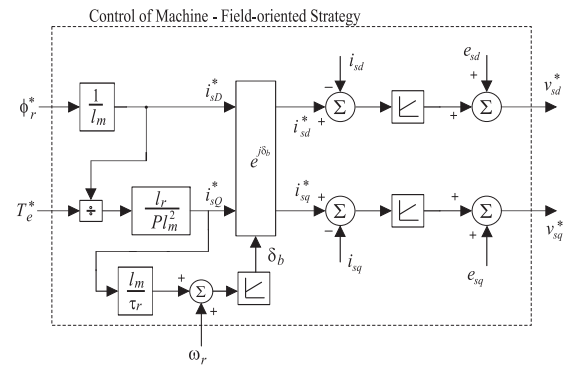
In this paper, a standard IFOC (Indirect Field Oriented Control) strategy has been considered for the three-phase machines, as observed in Fig. 3(c).

Indirect Field Oriented Control

For the indirect field oriented control, the three-phase machine control block [see Fig. 3(b)] the dq reference currents



(a)



(b)

Fig. 3. a) Control block diagram of the systems: YD-P and DD-P with $k \rightarrow 1$; YD-S with $k \rightarrow 2$. b) Three-phase machine control.

can be given by

$$i_{sd}^* = \frac{\phi_r^*}{l_m} \cos(\delta_e^*) - \frac{l_r}{Pl_m} \frac{T_e^*}{\phi_r^*} \sin(\delta_e^*) \quad (67)$$

$$i_{sq}^* = \frac{\phi_r^*}{l_m} \sin(\delta_e^*) - \frac{l_r}{Pl_m} \frac{T_e^*}{\phi_r^*} \cos(\delta_e^*) \quad (68)$$

$$\delta_b^* = \int_0^t \left(\frac{l_m}{\tau_r} \frac{i_{sq}^*}{\phi_r^*} + \omega_r \right) dt \quad (69)$$

where T_e^* , is the reference torque and $\phi_r^* = \phi_r^* e^{\delta_b^*}$ is the reference rotor flux vector. In the Fig. 3(b) e_{sd} and e_{sq} are the dq components of FEM, it is considered as perturbation for the control system.

VII. DC-LINK VOLTAGE COMPARISON

Given the model for the proposed configurations, the following equations can be written to compute the minimum required value of the dc-link voltage:

Configuration YD-P

$$E = |v_{1j} - v_{1k}| \quad j, k = a, b, c \text{ and } j \neq k \quad (70)$$

$$E = |v_{1j} - v_{1c} + v_{2k}| \quad j = a, b \text{ and } k = a, b, c \quad (71)$$

$$E = |v_{2k}| \quad k = a, b, c \quad (72)$$

Configuration DD-P

$$E = |v_{1j} + v_{2k}| \quad j = b, c \text{ and } k = a, c \quad (73)$$

$$E = |v_{1k}| \quad k = a, b, c \quad (74)$$

$$E = |v_{2k}| \quad k = a, b, c \quad (75)$$

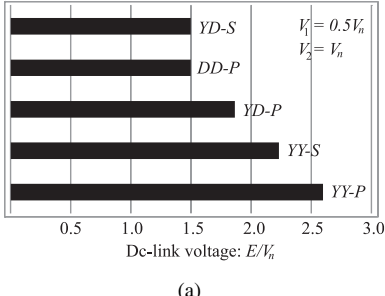
Configuration YD-S

$$E = |v_{1j} - v_{1k}| \quad j, k = a, b, c \text{ and } j \neq k \quad (76)$$

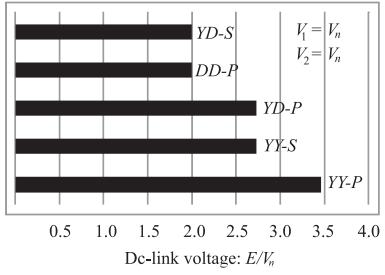
$$E = |v_{1j} + v_{2k}| \quad j = a, b, c \text{ and } k = a, c \quad (77)$$

$$E = |v_{2b}| \quad (78)$$

The proposed configurations present dc-link voltages lower than that configurations showed in Fig. 1, due to the Δ -connected arrangement. This is confirmed by Fig. 4, which shows the dc-link voltage demanded by configurations showed in Figs. 1 and 2. Notice that, even considering different voltage rated for machines 1 and 2, the proposed configurations presents lower dc-link voltage. In this figure V_n is the rated voltage.



(a)

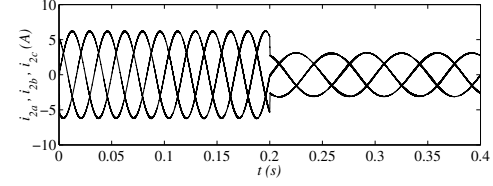
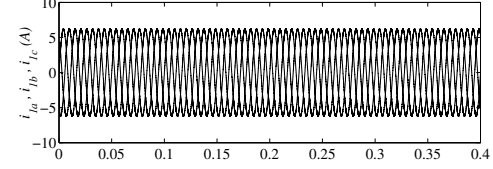


(b)

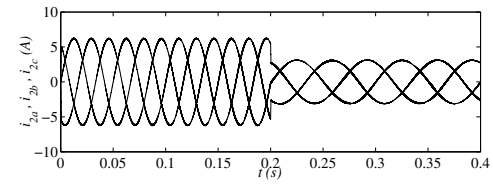
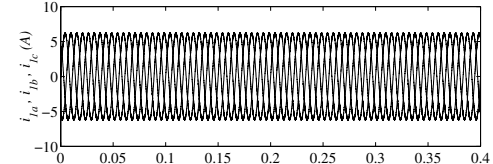
Fig. 4. Dc-link voltage demanded for each configuration considering different voltage for both machines. (a) $V_1 = 0.5V_n$ and $V_2 = V_n$. (b) $V_1 = V_2 = V_n$.

VIII. CONVERTER CURRENT COMPARISON

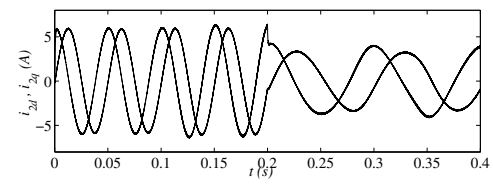
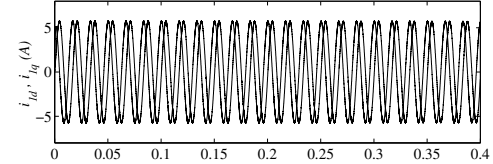
Table I shows the RMS current of the power switches for each configuration studied in this paper. In this table I_1 and I_2 means RMS phase current flowing through the machines 1 and 2, respectively. Notice that the currents in the switches of configuration with at least one machine in a delta connection are higher than that with wye connection.



(a)



(b)



(c)

Fig. 5. Simulation results of currents of machine 1 (top) and machine 2 (bottom). (a) Phase currents of machines of Configuration YD-P. (b) Phase currents of machines of Configuration DD-P. (c) dq currents of machines of Configuration YD-S.

TABLE I
MACHINES PAREMETERS.

Configuration	q_1/q_2	q_3	q_4/q_5
YY-P	I_1	$I_1 + I_2$	I_2
YY-S	$I_1 + \frac{I_2}{3}$	$I_1 + \frac{I_2}{3}$	I_2
YD-P	I_1	$I_1 + \sqrt{3}I_2$	$\sqrt{3}I_2$
DD-P	$\sqrt{3}I_1$	$\sqrt{3}(I_1 + I_2)$	$\sqrt{3}I_2$
YD-S	$I_1 + \frac{I_2}{\sqrt{3}}$	$I_1 + \frac{I_2}{\sqrt{3}}$	$\sqrt{3}I_2$

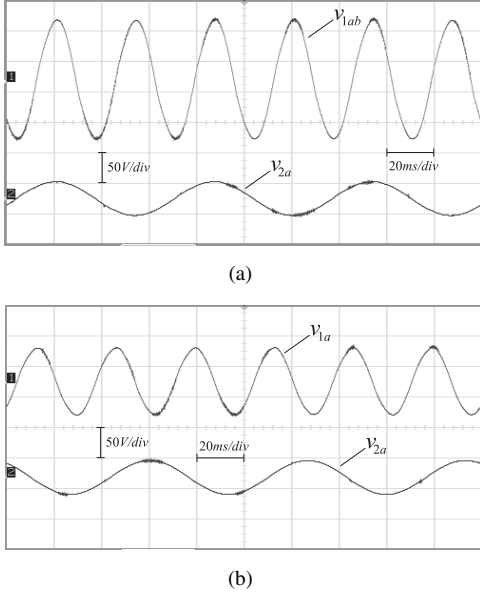


Fig. 6. Experimental results. (a) Line-to-line voltages of Machine #1 and Machine #2 for Configuration YD-P. (b) Line-to-line voltages of Machine #1 and Machine #2 for Configuration DD-P.

TABLE II
MACHINES PAREMETERS.

Parameter	Machine #1 and #2
R_s	8.7Ω
L_s	$0.02694H$
R_r	1.95Ω
L_r	$0.02694H$
L_m	$0.4849H$
N^o of poles	4
Moment of Inertia	0.00328

IX. SIMULATION RESULTS

In the simulation tests the switching frequency was $10kHz$ and the machines parameters are presented in Table II.

Figs. 5(a)-(c) show the behavior of currents of both machines when them have been submitted to a transient in the amplitude and frequency of the reference current. Figs. 5(a)-(c) are related to Configurations YD-P, DD-P and YD-S, respectively. The reference current of Machine #2 is changed in a step-down transient from $6.2A$ and $20Hz$ to $3.1A$ and $10Hz$ at $t = 0.2s$. As observed in the Fig. 5 even with a hard transient the control strategy guarantees both machines uncoupled.

X. EXPERIMENTAL RESULTS

The topologies presented in Fig. 2 have been implemented in the laboratory. In the experimental tests the switching frequency was $10kHz$ and the capacitance of the dc-link capacitor was $2200\mu F$. The dc-link voltage was obtained through the rectifier using a three-phase grid as primary energy of source. The set-up used in the experimental tests is based on a microcomputer (PC-Pentium) equipped with appropriate plug-in boards and sensors.

Fig. 6(a) shows the line-to-line voltages of Machine #1 ($v_{1ab} = v_{1a} - v_{1b}$) and Machine #2 (v_{2a}) for Configuration YD-P operating at $30Hz$ and $15Hz$, respectively. Fig. 6(b) shows the line-to-line voltages of Machine #1 (v_{1a}) and Machine #2 (v_{2a}) for Configuration DD-P operating also at $30Hz$ and $15Hz$, respectively. Notice that these waveforms were obtained using a low frequency filter.

XI. CONCLUSION

This paper proposes three configurations for supplying two three-phase ac motors with five legs. The five-leg inverter supplying independently two motors has been used as a potential solution for driving a traction motor and a compressor motor in automotive applications. Such five-leg inverter allows a reduction in the compressor drive cost. Overall comparison of the configurations favors the proposed configuration compared to the configurations found in the technical literature, especially in terms of dc-link voltage reduction.

REFERENCES

- [1] H. W. van der Broeck and J. D. van Wyk, "A comparative investigation of a three-phase induction machine drive with a component minimized voltage-fed inverter under different control options," *IEEE Trans. Ind. Appl.*, vol. 20, pp. 309–320, Mar./Apr. 1984.
- [2] F. Blaabjerg, S. Freysson, H. H. Hansen, and S. Hansen, "Comparison of a space-vector modulation strategy for a three phase standard and a component minimized voltage source inverter," in *Proc. EPE*, pp. 1806–1813, 1995.
- [3] C.-T. Pan and M.-C. Jiang, "Control and implementation of three phase voltage-double reversible AC to DC converter," in *Proc. IEEE PESC*, pp. 437–443, 1995.
- [4] C. B. Jacobina, M. B. R. Correa, E. R. C. da Silva, and A. M. N. Lima, "Induction motor drive system for low-power applications," *IEEE Trans. Ind. Appl.*, vol. 35, pp. 52–61, Jan./Feb. 1999.
- [5] P. Enjeti and A. Rahman, "A new single phase to three phase converter with active input current shaping for low cost AC motor drives," in *Conf. Rec. IEEE-IAS Annu. Meeting*, pp. 935–939, 1990.
- [6] G.-T. Kim and T. A. Lipo, "VSI-PWM rectifier/inverter system with a reduced switch count," in *Conf. Rec. IEEE-IAS Annu. Meeting*, pp. 2327 – 2332, 1995.
- [7] B. K. Lee, B. Fahimi, and M. Ehsani, "Overview of reduced parts converter topologies for AC motor drives," in *Proc. IEEE PESC*, pp. 2019–2024, 2001.
- [8] E. C. dos Santos Jr., C. B. Jacobina, H. A. Toliyat, and E. R. C. da Silva, "Monolithic systems using standard three-leg inverter supplying independently two motors," *IEEE Trans. Ind. Appl.*, vol. 45, pp. 1660–1669, Sep./Oct. 2009.
- [9] G. J. Su and J. S. Hsu, "An integrated traction and compressor drive system for ev/hev applications," in *Proc. IEEE APEC*, 2005.
- [10] G.-J. Su and J. S. Hsu, "A five-leg inverter for driving a traction motor and a compressor motor," *IEEE Trans. Power Electron.*, vol. 21, pp. 687–692, May 2006.
- [11] C. B. Jacobina, O. I. da Silva, E. C. dos Santos Jr., and A. M. N. Lima, "Dual ac drives with five-leg converter," in *Proc. IEEE PESC*, pp. 1800–1806, 2005.
- [12] C. B. Jacobina, O. I. da Silva, E. C. dos Santos Jr., A. M. N. Lima, and I. S. de Freitas, "AC drive systems using five-leg converter and series-connected machines," in *Proc. IEEE PESC*, pp. 2429–2435, 2005.
- [13] C. B. Jacobina, A. M. N. Lima, E. R. C. da Silva, R. N. C. Alves, and P. F. Seixas, "Digital scalar pulse-width modulation: a simple approach to introduce non-sinusoidal modulating waveforms," *IEEE Trans. Power Electron.*, vol. 16, pp. 351–359, May 2001.
- [14] V. Blasko, "Analysis of a hybrid PWM based on modified space-vector and triangle-comparison methods," *IEEE Trans. Ind. Appl.*, vol. 33, pp. 756–764, May/June 1996.